Lab on a Chip

Dynamic Article Links

Cite this: DOI: 10.1039/c2lc40311k

www.rsc.org/loc

PAPER

Direct-writing colloidal photonic crystal microfluidic chips by inkjet printing for label-free protein detection†

Weizhi Shen, Mingzhu Li,* Changqing Ye, Lei Jiang and Yanlin Song*

Received 5th December 2011, Accepted 24th May 2012
DOI: 10.1039/c2lc40311k

Integrating photonic crystals (PC) into microfluidic systems has attracted immense interest for its novel functions. However, it is still a great challenge to fabricate PC microfluidic chips rapidly with complex functions. In this work, a direct-writing colloidal PC microchannel was firstly achieved by inkjet printing and was used for the surface-tension-confined microfluidic immune assay. PC channels with different structure colors have been successfully integrated on one chip. The fabricated chip has the advantages of rapid fabrication, quick fluidic transport and can monitor the fluidic fluxion using the naked eye. Utilizing this PC microfluidic chip, a colorimetric label-free immune assay was realized without nonspecific adsorption interference of the target.

Introduction

Microfluidics has emerged as one of the fastest growing fields in chemical and biological applications.[1,2] The microfluidics system supports integrated functions including mixing, separation, optic/electric/thermo functions, detection and so on. Using novel functional materials to increase the functions and feasibility of the microfluidic devices has attracted immense interest. Photonic crystal (PC) materials are one of the attractive novel functional materials that can be incorporated into microfluidic devices and increase the potential capabilities of optics/photonics and microfluidics.[3–5] The PC has periodic variation of the dielectric permittivity at wavelength scale. Its photonic stop band is sensitive to the environmental refractive index. The superior properties of PC introduce many new functions into the microfluidic chips. The PC can act as not only an indicator of the fluid moving on the channel but also an on-chip label-free colorimetric sensor to specific analytes.[6] Moreover, the PC is adaptable and tunable to the microfluidic system,[7,8] which can introduce novel applications into the microfluidic devices such as the localized optical manipulation and response in channels.[9,10]

Several PC microfluidic devices have been fabricated through the photolithography.[11–15] Cunningham's group reported a two dimensional PC microfluidic well plate for combinatorial screening applications.[16] Yang's group utilized a novel holographic fabrication method[17] to fabricate a microfluidic chip with three dimensional PC and used it for a microfluidic passive mixing.[18,19] Assembling colloidal spheres in the microfluidic channel is another feasible method for constructing PC-microfluidic system.[20,21] Kim's group fabricated a microchannel with mechanically stable PC structures using assembled colloidal spheres, which largely increased the mixing efficiency in the microchannel.[22] Recently, Bettiol's group reported a colloidal PC as an optical filter for the microfluidic device.[23] However, these efforts based on the microfabrication or in-channel assembly methods are all hard to satisfy the demand of rapid and low-cost fabrication of photonic crystal microfluidic chip with complex functions.[24,25]

Inkjet printing is a popular technology being explored for many applications including microdispensing and assembly of materials.[26] It has been applied in the fabrication of optic/electric devices such as polymeric LED materials,[27,28] FET devices,[29] and refractive microlense arrays.[30] A major challenge in applying inkjet processes for directly writing materials is formulating suitable inks. The direct inkjet printing PC is more challenging, because it involves controlled-assembly of the colloidal spheres in the printing process.[31–34]

In this work, we inkjet-printed PC microfluidic chips and used the chip for label-free immune detection. In order to achieve a well-ordered assembly of PC spheres and regular channel shape, the printing substrate was coated with a hydrophobic polymer-nanoparticle layer, and the ink solvents with high-boiling-point, high-polarity and high-viscosity were used. PCs with different stop bands and functions were integrated on one chip by using the inkjet printing method. Detection probes can also be located on the microfluidic chip by inkjet printing. Thus, the printing method is more flexible and can achieve one-step fabrication of the PC microfluidic chips compared with traditional methods. The PC formed a native hydrophilic pattern on a hydrophobic coating layer and served as the surface-tension-confined channels[23,24] to guide the fluidic transport. Moreover, the PC

Beijing National Laboratory for Molecular Sciences (BNLMS), Key Laboratory of Organic Solids, Laboratory of New Materials, Institute of Chemistry, Chinese Academy of Sciences, Beijing, 100190, P. R. China. E-mail: mingzhu@iccas.ac.cn; ylsong@iccas.ac.cn; Fax: (+86) 10-82627566; Tel: (+86) 10-82627566

† Electronic supplementary information (ESI) available: Durability of the colloidal PC; polarity of the solvent; reflection spectra of the PC channels in air, water and diethanolamine; detection results of goat IgG as a negative control; description of the solvent polarity; a digital video which shows the PC channel monitoring the fluidic movement with structural color change. See DOI: 10.1039/c2lc40311k

channel has the ability of monitoring fluidic fluxion through colorimetric analysis which can be observed by the naked eye. Utilizing the chip, a prototype human IgG antigen-antibody colorimetric detection was achieved based on the responsive wavelength shift of photonic stop band. The Y-shape microfluidic chip simultaneously detected the target antigen with and without the antibody probe at the ends of the two branches, which successfully eliminated the interference of nonspecific adsorption in this detection.

Experimental

Materials and instruments

Hydrophobic SiO_2 nanoparticles Aerosil R202 (surface modified with polydimethylsiloxane) with average particle size of 14 nm were purchased from Evonik Degussa Co., Ltd. Polystyrene (M_w = 350 000) were purchased from Aldrich. Dichloromethane, formamide, and diethanolamine (CP) were purchased from Sinopharm Chemical Reagent Co., Ltd. Poly(styrene-methyl methacrylate-acrylic acid) (poly(St-MMA-AA)) colloidal spheres were synthesized from the monomers of styrene (St), methyl methacrylate (MMA) and acrylic acid (AA) by the emulsion polymerization method. Their diameters are 190 nm, 216 nm and 235 nm, respectively.[35] Their polydispersities are less than 0.5%. Human immunoglobulin G (IgG), goat IgG, mouse anti human IgG, and bovine serum albumin (BSA) were purchased from the Beijing Biosynthesis Biotechnology Co., Ltd.

The reflection spectra of the PCs were collected using a microscope (IX71, Olympus) and CCD spectrograph (Acton SP2300, Princeton Instrument) from the normal angle. The light source is a bromine tungsten lamp with an optical fiber. FE-SEM images were obtained on a JEOL JSM-6700F (Japan) scanning electron microscope at 3.0 kV. Contact angles were measured on an OCA20 contact-angle system (Dataphysics Co., Germany) at ambient temperature (25 °C) .

Preparation and characterization of colloidal PC microfluidic channels

The monodispersed poly(St-MMA-AA) nanospheres were synthesized by the emulsion polymerization method.[35] The colloidal sphere has a hydrophobic hard core (PSt) and a hydrophilic soft shell (PMMA-AA). This core-shell structure of the poly(St-MMA-AA) sphere facilitated the lattice arrangement during the printing process and made the PC patterns have mechanical strength and resistance to aqueous solution.[35] The diameters of the nanospheres are 190 nm, 216 nm and 235 nm respectively. The printing inks contain *ca.* 33% colloidal spheres and the mixture of formamide, diethanolamine and water as the solvent.

The preparation of PC microfluidic chip by inkjet printing includes three processes. First, the hydrophobic printing substrate is made by coating glass slides with a hydrophobic layer by dip-coating method (Scheme 1a and b). The hydrophobic layer is composed of polystyrene and hydrophobic silica nanoparticles. 1.0 g polystyrene granules (M_w = 350 000 g mol^{-1}, Aldrich), 0.6 g hydrophobic silica nanoparticles (Aerosil R202, average diameter of particles is 14 nm, Evonik Degussa Co.) and 30 mL dichloromethane were mixed and stirred for 30 min in a sealed bottle. Pre-cleaned glass slides were dipped into this sticky solution and pulled up at a speed of *ca.* 0.5 cm s^{-1} forming a hydrophobic pre-coating layer.[36]

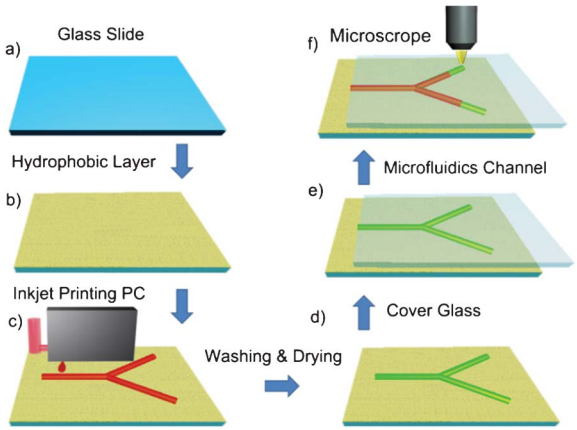

Scheme 1 The preparation of PC microfluidic chip by inkjet printing. (a) A hydrophobic substrate was prepared by coating a pre-cleaned glass slide with (b) a hydrophobic layer composed of polystyrene and hydrophobic SiO_2 nanoparticles. (c) Y-shape PC channel was inkjet printed on the substrate by using colloidal spheres dispersion as the ink. (d) The assembled PC pattern was washed to remove the residual ink solvents (e) and encapsulated with a cover glass. (f) The surface-tension-confined microfluidic chip was used for detection. A commercial inkjet dispenser system is used in the fabrication, so that the process is facile and rapid.

Then, the PicoSpot Jet Dispensing System (EFD, Inc.) was used for printing the microsphere ink on the hydrophobic substrate (Scheme 1c). Parameters of the inkjet system was optimized for a good printing performance. The dosage time was set to 0.25 ms, the pause time was set to 3.50 ms, and the pressure was set to 700 kpa. An XYZ 3D movement robot was used for locating the position of inkjet printing. The moving speed was set to 2 mm s^{-1}. The printed chips were dried in a chamber with 40% humidity and 40 °C. The Y-shape channel was printed on the chip, and three PC spots were printed on the three end points of the Y-shape channel. The spot at the stem end of the "Y" is for the fluidic injection and the spots at the two branch ends of "Y" are for the immune response. The Y-shape design of the PC chip is a demonstration of two-channel detections and satisfies the need of parallel detections. The spots and lines were printed with inks of different diameters colloidal spheres to form the PCs with different stop bands and show different structure colors.

Finally, the residual formamide and diethanolamine in the PC pattern were removed by carefully washing with pure water and drying with nitrogen stream (Scheme 1d). The colloidal PCs were stable, and the printed patterns remained good in the washing process due to merged soft shells between colloidal spheres (ESI, Fig. S1†).

Human IgG label-free immunoassay with the PC microfluidic chip

Utilizing the inkjet technique, the antibody mouse anti human IgG adsorbed on the end of the left branch channel with 1.0 mg ml^{-1} mouse anti human IgG solution over night at 37 °C. Then, the 5% BSA solution was inkjet-printed on both ends of the branch channels for blocking. The blocked spots were washed with a

solution of 0.01 M PBS with 3% Tween 20 through the PC channel. The left detection spot is for detecting the IgG adsorption to the anti IgG as the sample spot. The right spot without the anti IgG is used for eliminating the interference of the target's nonspecific adsorption as the control spot. The PC patterned chip was finally capped with 20 μm spacers and a cover glass, constructing the microfluidic chip for the prototype human IgG detection (Scheme 1e).

A series of human IgG solutions with different concentrations were detected by this PC microfluidic chip. The target solutions were injected from the spot at the end of the stem channel. With the capillary action, the solution drop rapidly spread following the PC pattern, and finally reached the two branch ends as the detection areas (Scheme 1f). The *in situ* reflection spectra of the PC detection spots were collected and monitored by the microscope system.

Results and discussions

Inkjet printing PC channels

The digital photographs and micrographs of PC channels have been shown in Fig. 1. The PC channels have different structural colors for utilizing the PC inks with different colloidal spheres (Fig. 1a and b). The green one is composed of colloidal spheres with the diameter of 216 nm (PC_{216}, Fig. 1a). The yellow one is composed of colloidal spheres with the diameter of 235 nm (PC_{235}, Fig. 1b). The width of PC_{216} is 380 μm and the width of the PC_{235} is 560 μm. In Fig. 1b, the three blue spots on the stem and branch ends of the yellow channel are composed of colloidal spheres with the diameter of 190 nm (PC_{190}). The blue spots were used as the injection and detection labels. The above results demonstrate that the inkjet printing provides a facile method to integrate different

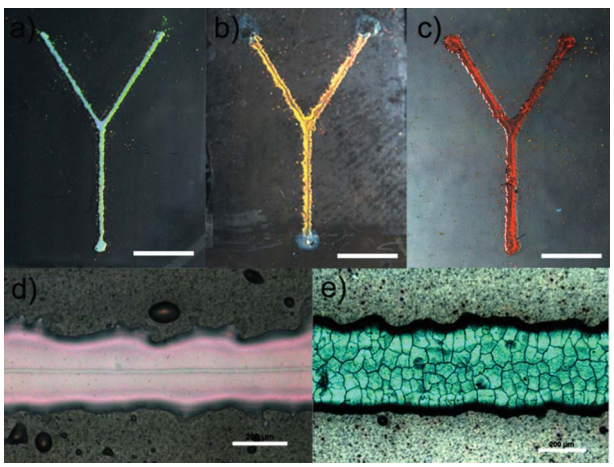

Fig. 1 (a, b, c) Digital photographs and (d, e) micrographs of PC chips. The Y-shape PC channels with (a) 216 nm (PC_{216}) and (b) 235 nm (PC_{235}) diameters colloidal spheres show structure colors as green and yellow, respectively. The three blue spots on the stem and branches ends of yellow channel are composed of colloidal spheres with the diameter of 190 nm (PC_{190}). (c) The unwashed PC_{216} channel shows a structure color as red with the residual ink solvents. The scale bars are 5 mm in (a), (b) and (c). The micrographs of the PC_{216} microchannel (d) before and (e) after washing off the residual formamide and diethanolamine (scale bar: 200 μm). The structure colors of the PC microchannel are red before washing and green after washing. The printed PC channels are smooth, regular and have multiple structural colors.

PCs on one chip as well as to achieve various fine patterns. The unwashed PC_{216} channel still has some residual ink solvents in its void and shows a structural color of red (Fig. 1c).

Fig. 1d and e show the micrographs of the PC_{216} channels before and after washing. The PC_{216} channel is red before washing and turns to green by washing off the residual ink solvent. It is clearly observed that the shapes of the channels are straight and regular. The high quality of the PC pattern is achieved by confining the spread of the PC ink. In the inkjet printing process, there is a large jetting force from the nozzle which can cause undesirable splashing and poor printing pattern. Therefore substrate and ink must be carefully tuned to prevent splashing. Firstly, the factors of the jetting including the pressure, the dosage time and so on are optimized. The jetting pressure is set as small as possible for precisely locating the ink drops.[26] The dosage time, pause time and moving speed of the dispensing valve are optimized coordinatively to control the printing drops distance. The printing distance between the former and latter drops were tuned to print a continuous liquid line on the substrate. The drops should not be too far away, which will form separate spots, and not be too close which will arise undesirable splashing. In the experiment, the jetting pressure was set to 700 kpa, the dosage time was set to 0.25 ms, the pause time was set to 3.50 ms, and the movement speed was set to 2 mm s^{-1}. Secondly, the properties of the substrate were modified by coating a hydrophobic layer. A hydrophobic polymer-nanoparticles composite film of polystyrene and SiO_2 nanoparticles was used for a hydrophobic and rough substrate. The ratio between PS and hydrophobic SiO_2 nanoparticles was set to 1 : 0.6 . The contact angle of the layer was tuned to 125.8 $\pm$ 2.1° (Fig. 4c), so that it is large enough to confine the spread of the ink. At the same time, the roughness of the substrate is tuned to be high enough to stick the drops on the substrate when they were merging together to be a line. Finally, the ink properties are adjusted by using proper solvents. The ink should have high boiling point, high polarity, high viscosity so as to facilitate the assembly of PC structure and the form of regular printing pattern. The solvent of the ink is made from the mixture of formamide (T_b = 210 °C) and diethanolamine (T_b = 269 °C), which can slow down the evaporation and overcome the "coffee ring effect".[34] The formamide was proved to be a successful solvent with high polarity (E_T^N= 0.775, the normalized E_T (30) (kcal mol^{-1}) value with reference to water (E_T^N = 1) and tetramethylsilane (E_T^N = 0), ESI, S2†)[37] for ordered assembly of colloidal spheres and resisting the coffee ring effect.[32] The diethanolamine has a high viscosity (351.9 mPa·s, 30 °C) for the thickening agent. Moreover, they barely screen the surface charge of the colloidal spheres and have little impact on the ordered assembly of colloidal PC.

The structural colors of PC patterns were dramatically changed in the printing and detection process because of the changing of environmental reflective index. Fig. 2 shows the reflection spectra of the PC channels from the normal angle (Fig. 2). When the ink was printed on the substrate and then dried for the assembly of colloidal spheres, the structural colors of PC channels were inconspicuous and their reflectivities were less than 0.1 (ESI, Fig. S3†). This was because formamide and diethanolamine were filling in the space of the PC structure. The refractive indices of the formamide (1.45) and diethanolamine

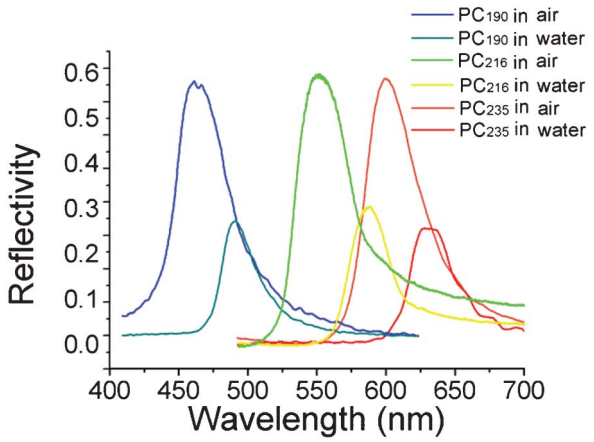

Fig. 2 Reflection spectra of PCs with the colloidal spheres diameters of 190 nm (PC_{190}), 216 nm (PC_{216}) and 235 nm (PC_{235}) with the air and the water. The reflection peaks of PCs red shift (from 463 nm, 552 nm and 599 nm to 492 nm, 590 nm and 632 nm for PC_{190}, PC_{216} and PC_{235}, respectively) and decrease (reflectivity from 0.6 to 0.25) when channels are wetted by aqueous solution. The PC channel can monitor the fluidic fluxion through the change of structural color.

(1.48) are close to that of the polymer spheres (1.59). Then, the chips were washed by water and dried. The space of PC structure was filled with air, which make the structural color turn bright. The refractive index contrast between the air and colloidal spheres became large (1.0 to 1.59), so that the reflectivity of the stop band sharply increased to *ca.* 0.6. The reflection peaks obviously blue shift due to the decrease of the effective refractive index of the PC. To more clearly understand the changes of the photonic stop band, further explanation is given as follows: the wavelengths of photonic stop bands are responsive to the environments and protein adsorption, which can be explained by Bragg's Law.

$$\lambda = 1.633d \times \sqrt{f_{\text{space}} \times n^2_{\text{space}} + f_{\text{protein}} \times n^2_{\text{sprotein}} + f_{\text{sphere}} \times n^2_{\text{sphere}}} \quad (1)$$

In eqn (1), the n_{space}, n_{protein}, and n_{sphere} are refractive indices of space between the colloidal spheres, adsorbed proteins, and PC sphere, respectively. The n_{sphere} and n_{protein} are fixed at their typical bulk values as $n_{\text{sphere}} = n_{\text{polystyrene}} = 1.59$, $n_{\text{protein}} = 1.42$, and n_{space} is changed from $n_{\text{water}} = 1.33$ to $n_{\text{air}} = 1.0$. The f_{space}, f_{protein}, and f_{sphere} are the volume fractions of water/air, protein and polystyrene spheres, respectively. As Fig. 2 shown, the intensities of reflection peaks decrease from *ca.* 0.6 to *ca.* 0.25, and wavelengths of these red shift when the PC channels are wetted by aqueous fluid. The initial wavelengths of reflection peaks (λ) are 463 nm, 552 nm and 599 nm for PC_{190}, PC_{216} and PC_{235}, respectively. The wetted PC channels have the reflection peaks wavelengths (λ) at 492 nm, 590 nm and 632 nm for PC_{190}, PC_{216} and PC_{235}, respectively. The average red shift of the stop band wavelength is *ca.* 33 nm for the three PC channels. The fluxion process of the aqueous solution with sharp color changes can be monitored by the naked eye (ESI, video S1†).

Characterization of PC channels

The cross-section and top-view SEM were shown in Fig. 3. The thickness of the PC channel is *ca.* 7.8 μm, and the width of the

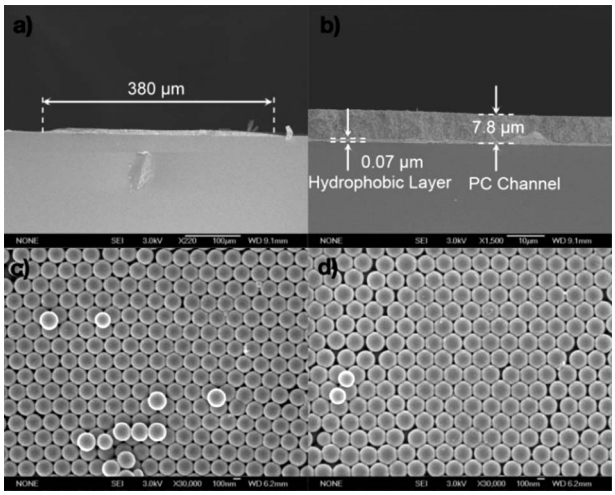

Fig. 3 (a, b) Cross-view and (c, d) top-view SEM of the PC channel. Cross-view SEM show the PC channel was (a) 380 μm wide and (b) 7.8 μm thick. The thickness of polystyrene-SiO_2 nanoparticles hydrophobic layer is around 0.07 μm. The (c) PC_{216} and (d) PC_{235} channels have high-ordered structures. The highly-ordered period structure and proper thickness play a key role in the bright structural color of the PC channel.

channel is *ca.* 380 μm (Fig. 3a and b). The channel width which is important for the velocity of fluidic transport can be controlled from 200–500 μm by the dosage time and pause time in the printing procedure. The thickness of the PC channel affects the absorption of the fluid as well as the PC's stop band. The absorption of PC channel to fluid relates to the capillary force in the porous nano structure of the colloidal PC and accelerates the movement speed of fluid in the suface-tension-confined channel. The thickness is determined by the surface tension and concentration of the PC ink. In the experiment, of PC is about *ca.* 32 layers colloidal spheres and 7.8 μm in thickness, which has been proved an optimized thickness for a good optical property of the PC. The top-view SEM images (Fig. 3c and d) show a high-ordered face-centered cubic (fcc) crystals with their (111) direction perpendicular to the substrate. The colloidal sphere diameters are *ca.* 216 nm for the PC_{216} (Fig. 3d) and *ca.* 235 nm for the PC_{235} (Fig. 3d). The assembly of colloidal spheres was controlled by the evaporation speed of the ink solvent. The high-polarity solvent (mixture of formamide and diethanolamine) barely screens the surface charge (negative, carboxyl group) of the colloidal spheres. The electrostatic repulsion between the colloidal spheres can balance the compelled aggregation when the solvent was slowly evaporated, resulting in the high-ordered assembly of colloidal spheres. The ink solvent is made from the mixture of formamide (T_b = 210 °C) and diethanolamine (T_b = 269 °C) and has high-boiling-point. Thus, the colloidal spheres can assemble into high-ordered period structure, which gives rise to PC patterns with quality stop bands (Fig. 2) and bright structural colors (Fig. 1).

In this work, the PC surface-tension-confined microfluidic chip is achieved by integrating a series of PCs through an inkjet printing method. As shown in Fig. 4a, the fresh-prepared PC channels were firstly washed with the pure water to remove the residual ink solvent. The water drops dewet from the hydrophobic substrate and spontaneously wet the Y-shape hydrophilic

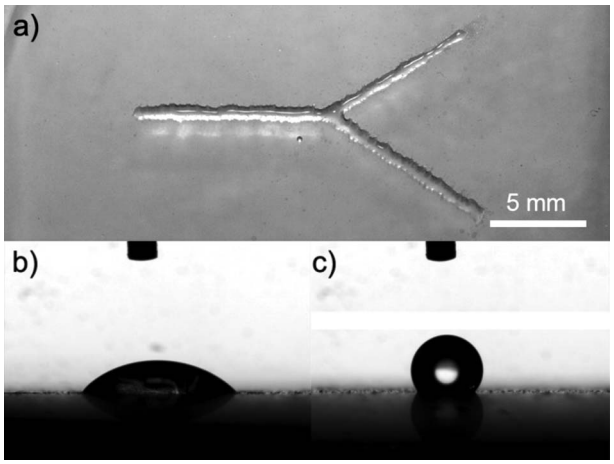

Fig. 4 (a) The wetting pattern of the water on the PC channel and the contact angles of water drops on (b) the PC channel and (c) hydrophobic coating (syringe needle diameter is 0.5 mm). The contact angle of the hydrophilic PC channel is 57.8 ± 2.5°and the contact angle of the hydrophobic coating layer is 125.8 ± 2.1°. The surface tension difference of the PC pattern and hydrophobic substrate are large enough for confining the water in the channel.

PC patterns (Fig. 4a). It is a visualized evidence of the hydrophoblic-hydrophilic difference pattern formed by the direct inkjet printing of PC. Hydrophilic–hydrophobic pattern is attractive in the surface wettability researches and has great potential applications in printing press and microdevices fabrication.[39,48] The surface-tension-confined microfluidic strategy is to confine fluids[39] and realize the liquid transport through the surface tension by utilizing the hydrophobic-hydrophilic pattern on the surface.[40] A parallel-plate configured device is capable of supporting fluidic transport through capillarity, which is called the ''surface-tension-confined microfluidics''.[41,42] The surface-tension-confined microfluidic device can be fabricated easily using the inkjet printing technique with hydrophilic inks.[43] In virtual surface-tension-confined microfluidic devices, multiple functions have been proved such as chemical reactions,[44] spontaneous oscillating liquid transport,[45] passive micromixing[46] and sensitive SERS detection.[47] For the prepared PC microfluidic chip, the PC patterns are native hydrophilic channels on the hydrophobic substrate. The PC patterns are hydrophilic because the poly(styrene-methyl methacrylate-acrylic acid) colloidal spheres have large amount of carboxyl groups on their surface from the poly acrylic acid component.[38] Moreover, the porous structure makes the PC channel capable of absorbing the fluid. The substrate is hydrophobic due to the hydrophobic coating of polystyrene–SiO_2. Thus, prepared PC microfluidic chip is a surface-tension-confined microfluidic chip. The contact angles of 2 μL water drops on the PC channel and the hydrophobic coating layer are *ca.* 57.8 ± 2.5° (θ_a) and 125.8 ± 2.1° (θ_b), respectively (25 °C, Fig. 3b and c). The confining force supported from this PC channel can be approximated by the unbalance Young's force,[49] F_Y, which results from the difference in wettability or surface energy between the in-channel-side and out-channel-side of the drop when it is going to diverge from the channel:

$$F_Y = \gamma_w (\cos\theta_a - \cos\theta_b) \quad (2)$$

where γ_w is the surface tension of the water. The F_Y is *ca.* 78.1 mN m^{-1}. Thus, the surface tension difference between the hydrophilic PC channel and hydrophobic is large enough for a surface-tension-confined fluidic channel.[42]

So far as we know, our chip is the first surface-tension-confined PC microfluidic chip which has advantages of rapid fabrication, quick fluidic transport, and monitoring the fluidic fluxion with the naked eye (ESI, video S1†). The aqueous solution flows along the PC pattern with the pulling and confining force from the capillarity and surface tension. Simultaneously, the solution wets the PC channel, which changes the refractive index of the environment from 1.0 (air) to 1.33 (water). Thus, the PC stop band can respond to this refractive index changing, showing different structural colors. This property of the PC channel makes the microfluidic operation visible and will be useful for practical devices.

Label-free detection of human IgG

The surface-tension-confined PC chip is used for a label-free immune assay. The left branch end of the PC chips were modified with the mouse anti human IgG and BSA serving as the sample spot, and the right one modified with the BSA serving as the control spot (Fig. 5a). During the probe modification process, the wavelength of PC reflection peaks take shifts assigned to the adsorption of the anti IgG and the BSA, shown in Fig. 5b. The original reflection peak wavelengths are at 583.42 nm for the sample spot and 595.48 nm for the control spot. The difference of the initial wavelengths between the sample and control spot arises from the deviation of the PC structure at different detection area. The reflection peak wavelength of the sample spot red shifts to 585.47 nm after the mouse anti human IgG modification. With BSA blocking, the final wavelengths of reflection peaks reach 587.34 nm for the sample spot and 598.50 nm for the control spot. The total red shifts of the sample and the control spots are 3.92 nm and 3.02 nm, respectively. The stop band wavelength is sensitive to the refractive index change of the environment. The *in situ* colorimetric detections were carried out by collecting the reflection spectra at the same area of the PC microfluidic chip. The shift of the reflection peak corresponding to the protein binding can be used for quantitatively estimating the amount of bound protein. So a complete blocking of the surface can be proved by the shift.[6] Then, the target protein human IgG solutions with series concentrations (0–10 mg ml^{-1}) were injected into the stem of the Y-shape channel and flowed along the channel to reach the both branch ends. At the detection spot, the *in situ* reflection spectra of the sample spot and control spot were collected (Fig. 5a). The wavelengths (λ) of reflection peaks corresponding to various human IgG concentrations are shown in Fig. 5c. The initial wavelength of the sample spot is 587.34 ± 0.08 nm and that of the control spot is 598.38 ± 0.09 nm. It is seen that the wavelength of reflection peaks red shift for both of the sample spot and the control spot with the increase of the human IgG concentrations. The final wavelengths for 10.0 mg ml^{-1} target solution shift 6.02 nm for the sample spot and 4.11 nm for the control spot. The reflection wavelength of the sample spot gets to 593.54 ± 0.08 nm and that of the control spot gets to 602.50 ± 0.07 nm. However, the wavelength-concentration

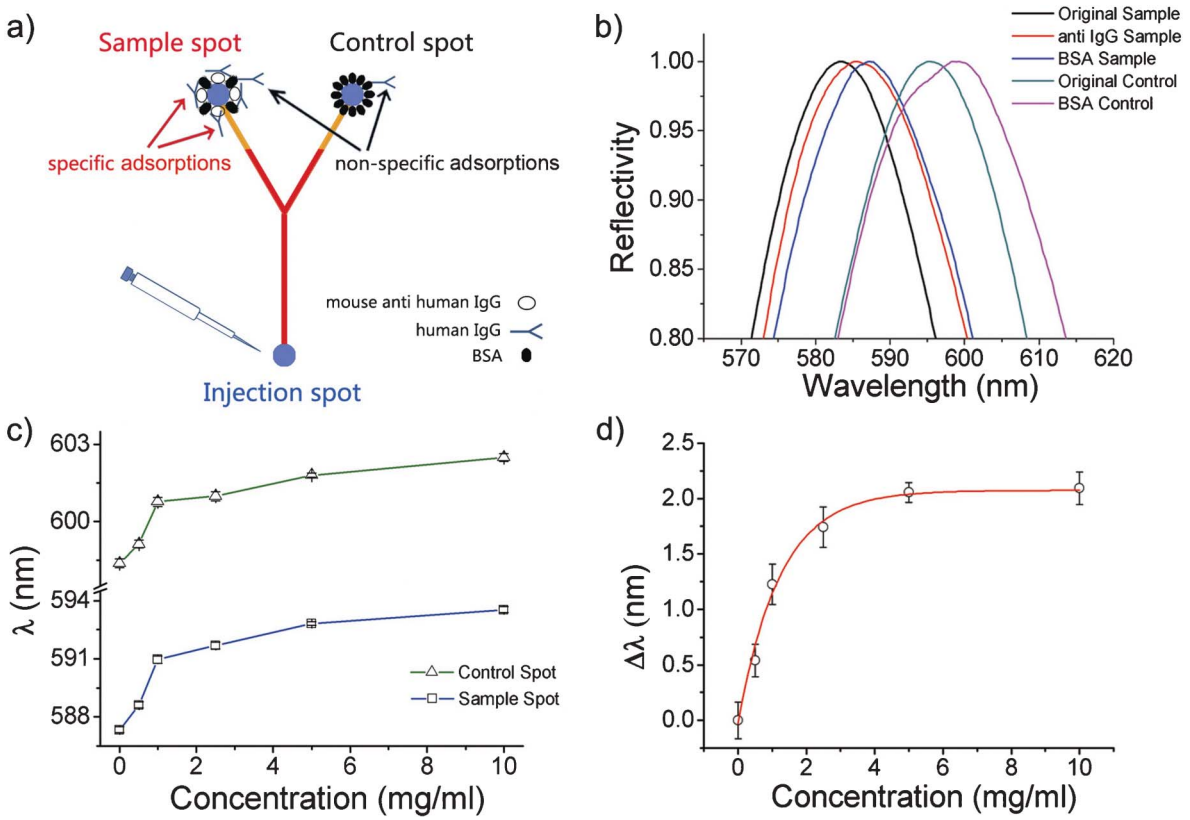

Fig. 5 (a) Schematic drawing of the Y-shape PC chip and the functional modifications. (b) The *in situ* reflection spectra of the sample spot and the control spot with the mouse anti human IgG (anti IgG) modification and BSA blocking. The peak wavelengths are red shifted *ca.* 3.92 nm and 3.02 nm for the sample and control spots, demonstrating a complete surface blocking. (c) The raw detection results (reflection peak wavelengths, λ) of the sample and control spots for series concentrations of IgG solutions (0–10 mg ml^{-1}). The response shifts of the control spot arise from the nonspecific adsorption of the target. The detection curves are not regular and hardly fit the exponential function. (d) The normalized detection results ($\Delta\lambda$) are computed from differences between the sample spot and control spot data to eliminate the interference of IgG's nonspecific adsorption. It fits the exponential function well. The error bars are summed deviations of the sample and control spots.

relationship curve is rough and irregular, and hardly fits the exponential function. Meanwhile, the control detection result is undesirable response to the concentration increase of target human IgG. This result is ascribed to the nonspecific adsorption of the IgG, resulting from insufficient washing in the channel detection. Therefore, we defined the result of the control spot as the nonspecific adsorption control in this microfluidic detection, and used it to correct the result of the sample spot. The result of sample spot subtracted the that of control spot for the nonspecific-adsorption-free detection result ($\Delta\lambda$), which has been normalized as shown in Fig. 5d. The detection error of normalized result is the sum of the detection errors of the sample spot and the control spot (Fig. 5d). The total wavelength shift of the normalized result ($\Delta\lambda$) is *ca.* 2.09 $\pm$ 0.15 nm from the target concentration of 0 mg ml^{-1} to 10.0 mg ml^{-1}. The normalized result fits well with the exponential function, and shows sensitive response to the IgG concentration in the range from 0 mg ml^{-1} to 2.5 mg ml^{-1}. A goat IgG solution is also detected on this PC microfluidic chip as a control detection sample. The goat IgG cannot be immune recognized by the mouse anti human IgG, which only gives a nonspecific adsorption both on the sample and control spot. Thus, the normalized result ($\Delta\lambda$) of goat IgG detection is negative (ESI, Fig. S4†). Therefore, the detection is specific to the specific antibody probe. It is proved that the Y-shape PC microfluidic chip can be used for a label-free colorimetric detection of IgG. Moreover, it successfully eliminates the background interference of nonspecific adsorption by *in situ* carrying on the detections of the sample spot and the control spot. This is a novel function which the film PC cannot do. It is also a demonstration of PC microfluidic chip with the capability of multi-channel experiment.

Conclusions

In conclusion, a PC microfluidic chip has been fabricated by the inkjet printing method. The inkjet printing provides a facile approach for the integration of different PCs on one chip. The prepared chips have advantages of rapid fabrication and quick fluidic transport. Moreover, the PC pattern is native hydrophilic channel on the hydrophobic substrate which can act as a feasible and novel surface-tension-confined PC microfluidics device. At the same time, the PC channels have the capability of monitoring the fluidic fluxion, and the prepared chip can be used to realize label-free detection through colorimetric analysis. In this work, a label-free detection chip with Y-shape PC channel realizes eliminating interference of nonspecific-adsorption in the label-free human IgG detection. The PC microfluidic chip can reduce the risk of contamination, be operated easily, and have high reliability and efficiency. The result indicates that the inkjet

printing provides a low-cost, facile and feasible approach to integrate colloidal photonic crystals with microfluidics, which can enlarge the fabrication methods and the functions of microfluidic system. We believe this result will largely facilitate the applications of PCs for optofluidics analysis, and wide-scale deployment of microfluidic "lab on a chip" technologies. The colloidal PC has superior ability of tunable wettability for microfluidic manipulation and responsive photonic stop band for optical analysis. Utilizing the optimal design of different patterns and functional modification, more complex microfluidic system or microarray with colloidal PCs can be fabricated by the inkjet printing method, which are engaged in our next work.

Acknowledgements

This work is supported by the National Nature Science Foundation (Grant Nos. 21003132, 21073203, 21004068, 91127038, 51103004 and 51173190), and the 973 Program (2007CB936403, 2009CB930404, 2011CB932303 and 2011CB808400).

References

1 J. S. Kuo and D. T. Chiu, *Lab Chip*, 2011, **11**, 2656–2665.
2 M. I. Mohammed and M. P. Desmulliez, *Lab Chip*, 2011, **11**, 569–595.
3 D. Erickson, X. Serey, Y. F. Chen and S. Mandal, *Lab Chip*, 2011, **11**, 995–1009.
4 S.-H. Kim, J. W. Shim and S.-M. Yang, *Angew. Chem., Int. Ed.*, 2011, **50**, 1171–1174.
5 D. Psaltis, S. R. Quake and C. Yang, *Nature*, 2006, **442**, 381–386.
6 W. Qian, Z.-Z. Gu, A. Fujishima and O. Sato, *Langmuir*, 2002, **18**, 4526–4529.
7 Y. Zhao, X. Zhao, J. Hu, M. Xu, W. Zhao, L. Sun, C. Zhu, H. Xu and Z. Gu, *Adv. Mater.*, 2009, **21**, 569–572.
8 C. Sun, X.-W. Zhao, Y.-J. Zhao, R. Zhu and Z.-Z. Gu, *Small*, 2008, **4**, 592–596.
9 S.-K. Lee, S.-H. Kim, J.-H. Kang, S.-G. Park, W.-J. Jung, S.-H. Kim, G.-R. Yi and S.-M. Yang, *Microfluid. Nanofluid.*, 2007, **4**, 129–144.
10 S. J. Williams, A. Kumar and S. T. Wereley, *Lab Chip*, 2008, **8**, 1879–1882.
11 P. S. Nunes, N. A. Mortensen, J. P. Kutter and K. B. Mogensen, *Sensors*, 2010, **10**, 2348–2358.
12 C. J. Choi and B. T. Cunningham, *Lab Chip*, 2006, **6**, 1373–1380.
13 C. J. Choi and B. T. Cunningham, *Lab Chip*, 2007, **7**, 550–556.
14 P. S. Nunes, N. A. Mortensen, J. P. Kutter and K. B. Mogensen, *Opt. Lett.*, 2008, **33**, 1623–1625.
15 J. Wu, D. Day and M. Gu, *Appl. Phys. Lett.*, 2008, **92**, 071108.
16 B. R. Schudel, C. J. Choi, B. T. Cunningham and P. J. Kenis, *Lab Chip*, 2009, **9**, 1676–1680.
17 S. K. Lee, H. S. Park, G. R. Yi, J. H. Moon and S. M. Yang, *Angew. Chem., Int. Ed.*, 2009, **48**, 7000–7005.
18 S. K. Lee, S. G. Park, J. H. Moon and S. M. Yang, *Lab Chip*, 2008, **8**, 388–391.
19 S. G. Park, S. K. Lee, J. H. Moon and S. M. Yang, *Lab Chip*, 2009, **9**, 3144–3150.
20 E. Kim, Y. Xia and G. M. Whitesides, *Adv. Mater.*, 1996, **8**, 245–247.
21 G. A. Ozin and S. M. Yang, *Adv. Funct. Mater.*, 2001, **11**, 95–104.
22 Z. Xiao, A. Wang, J. Perumal and D.-P. Kim, *Adv. Funct. Mater.*, 2010, **20**, 1473–1479.
23 S.-K. Hoi, X. Chen, V. S. Kumar, S. Homhuan, C.-H. Sow and A. A. Bettiol, *Adv. Funct. Mater.*, 2011, **21**, 2847–2853.
24 J.-Y. Shiu, C.-W. Kuo and P. Chen, *J. Am. Chem. Soc.*, 2004, **126**, 8096–8097.
25 J. Y. Shiu and P. Chen, *Adv. Mater.*, 2005, **17**, 1866–1869.
26 E. Duqi, M. Bocchi, L. Giulianelli, N. Pecorari, E. Franchi Scarselli and R. Guerrieri, *Sens. Actuators, A*, 2011, **168**, 320–327.
27 E. Tekin, P. J. Smith, S. Hoeppener, A. M. J. van den Berg, A. S. Susha, A. L. Rogach, J. Feldmann and U. S. Schubert, *Adv. Funct. Mater.*, 2007, **17**, 23–28.
28 G. Mauthner, K. Landfester, A. Köck, H. Brückl, M. Kast, C. Stepper and E. J. W. List, *Org. Electron.*, 2008, **9**, 164–170.
29 Y. Liu, K. Varahramyan and T. Cui, *Macromol. Rapid Commun.*, 2005, **26**, 1955–1959.
30 C.-T. Chen, C.-L. Chiu, Z.-F. Tseng and C.-T. Chuang, *Sens. Actuators, A*, 2008, **147**, 369–377.
31 H. Kim, J. Ge, J. Kim, S.-e. Choi, H. Lee, H. Lee, W. Park, Y. Yin and S. Kwon, *Nat. Photonics*, 2009, **3**, 534–540.
32 H.-Y. Ko, J. Park, H. Shin and J. Moon, *Chem. Mater.*, 2004, **16**, 4212–4215.
33 J. Park, J. Moon, H. Shin, D. Wang and M. Park, *J. Colloid Interface Sci.*, 2006, **298**, 713–719.
34 L. Cui, Y. Li, J. Wang, E. Tian, X. Zhang, Y. Zhang, Y. Song and L. Jiang, *J. Mater. Chem.*, 2009, **19**, 5499–5502.
35 J. Wang, Y. Wen, H. Ge, Z. Sun, Y. Zheng, Y. Song and L. Jiang, *Macromol. Chem. Phys.*, 2006, **207**, 596–604.
36 B. Su, S. Wang, Y. Song and L. Jiang, *Nano Res.*, 2010, **4**, 266–273.
37 K. Herodes, I. Leito, I. Koppel and M. Rosés, *J. Phys. Org. Chem.*, 1999, **12**, 109–115.
38 J. Wang, Y. Zhang, S. Wang, Y. Song and L. Jiang, *Acc. Chem. Res.*, 2011, **44**, 405–415.
39 L. Zhai, M. C. Berg, F. Ç. Cebeci, Y. Kim, J. M. Milwid, M. F. Rubner and R. E. Cohen, *Nano Lett.*, 2006, **6**, 1213–1217.
40 H. Gau, S. Herminghaus, P. Lenz and R. Lipowsky, *Science*, 1999, **283**, 46–49.
41 P. Lam, K. J. Wynne and G. E. Wnek, *Langmuir*, 2002, **18**, 948–951.
42 M. J. Swickrath, S. Shenoy, J. A. Mann, J. Belcher, R. Kovar and G. E. Wnek, *Microfluid. Nanofluid.*, 2007, **4**, 601–611.
43 M. Watanabe, *Microfluid. Nanofluid.*, 2010, **8**, 403–408.
44 A. Nag, B. Panda and A. Chattopadhyay, *Pramana*, 2005, **65**, 621–630.
45 S.-h. Chao and D. R. Meldrum, *Lab Chip*, 2009, **9**, 867–869.
46 M. J. Swickrath, S. D. Burns and G. E. Wnek, *Sens. Actuators, B*, 2009, **140**, 656–662.
47 B. D. Piorek, S. J. Lee, J. G. Santiago, M. Moskovits, S. Banerjee and C. D. Meinhart, *Proc. Natl. Acad. Sci. U. S. A.*, 2007, **104**, 18898–18901.
48 B. Su, S. Wang, J. Ma, Y. Song and L. Jiang, *Adv. Funct. Mater.*, 2011, **21**, 3297–3307.
49 M. K. Chaudhury and G. M. Whitesides, *Science*, 1992, **256**, 1539–1541.